RSC Advances

ROYAL SOCIETY OF CHEMISTRY

www.rsc.org/advances

1 **In situ synthesis of a bio-cellulose/titanium dioxide nanocomposite by using a**

2 **cell-free system**

3 Muhammad Wajid Ullah[1], Mazhar Ul-Islam[1,2], Shaukat Khan[1], Yeji Kim[1], Jae Hyun Jang[1],

4 Joong Kon Park[1]*

5 [1]Department of Chemical Engineering, Kyungpook National University, Daegu 702-701, Korea

6 [2]Department of Chemical Engineering, College of Engineering, Dhofar University, Salalah, 211,

7 Oman

8
9
10
11
12
13
14

15 ***Corresponding author**

16 **Joong Kon Park**

17 **Email:** parkjk@knu.ac.kr

18 Phone: +82539505621

19 Fax: +82539506615

Abstract

In the current study, nanocomposites of bio-cellulose with titanium dioxide nanoparticles (TiO_2-NPs) were synthesized by an in situ strategy using a cell-free system. The system was developed from *Gluconacetobacter hansenii* PJK through bead beating. A suspension of TiO_2-NPs was prepared in 1% sodium dodecyl sulfate and added to the cell-free extract of *G. hansenii* PJK. The bio-cellulose/TiO_2 nanocomposite was synthesized at 30°C, pH 5.0 for 5 days (bio-cellulose/TiO_2-I), 10 days (bio-cellulose/TiO_2-II), and 15 days (bio-cellulose/TiO_2-III) using 10 g/L glucose. Field-emission scanning electron microscopy (FE-SEM) confirmed the structural features and impregnation of TiO_2-NPs into the bio-cellulose matrix. Fourier transform-infrared (FT-IR) spectroscopy confirmed the presence of Ti-O groups in the chemical structure of the nanocomposite. X-ray diffraction (XRD) analysis indicated the presence of specific peaks for bio-cellulose and TiO_2-NPs in the nanocomposite. The TiO_2-NPs uptake by bio-cellulose was greatly increased with time and $40 \pm 1.6\%$ of the initially added nanoparticles were successfully impregnated into the nanocomposite after 15 days of incubation. NPs release analysis revealed minute detachment though a prolonged treatment time of 10 days. The synthesized nanocomposite showed better thermal and mechanical properties compared to pure bio-cellulose. The antibacterial test revealed impressive results where the inhibition zones produced against *E. coli* by bio-cellulose, bio-cellulose/TiO_2-I, bio-cellulose/TiO_2-II, and bio-cellulose/TiO_2-III were zero, 2.1 cm, 2.5 cm, and 3.7 cm, respectively. The current strategy can be effectively employed for the development of composite materials of biopolymers with several kinds of bactericidal elements.

Introduction

Biopolymers are extensively used as support materials for various applications due to their excellent physico-mechanical and biological properties. However, their widespread applications in biomedical research are limited due to their lack of bactericidal properties. This inadequacy has been overcome through the development of polymers-nanomaterials composites.[1,2] In such composites, the polymer serves as a support material while the inorganic nanoparticles act as a reinforcement material that possess the bactericidal properties.[1,3] These nanocomposites have shown impressive magnetic, electrical, catalytic, optical, and biological properties.[4,5] Several types of nanoparticles have been reported for the development of nanocomposites such as metals (Ag, Au, etc.) and metal oxides (ZnO, TiO_2, CoO, MgO, CaO, NiO, etc.).[1,2] Among these, the TiO_2 nanoparticle is a multifunctional metal oxide that has received immense consideration owing to its unique structural, thermal, electronic, optical, and antibacterial properties. Recent investigations have shown great potential for the application of TiO_2 nanoparticles in the areas of photovoltaics, photocatalysis, photoelectrochromics, and sensor development.[2,6] Further, TiO_2 is considered a safe material for application in sunscreens, ointments, and toothpastes due to it being non-toxic to animal and human cells.[2]

Microbial cellulose, a biopolymer produced by several microbial species, has received immense consideration owing to its purity, improved physico-mechanical, and biological properties.[7,8] It serves as a carrier in drug delivery systems, enzyme immobilization, and scaffold for tissue engineering, which further highlights its importance in several fields.[9-11] Furthermore, it possesses a high potential to form composites with most biocompatible and bactericidal elements.[9,12,13] Microbial cellulose is composed of a fibrous structure where thin fibrils are interconnected through inter- and intra-molecular hydrogen bonding that stabilize its reticulate

64   structure.[14] The fibrils are loosely arranged with empty spaces between them that result in

65   expanded surface area and a highly porous matrix.[15-17] Further, the strong and stable fibrils offer

66   better resistance to applied force and resist any variation in its structure. Similarly, the empty

67   spaces between the fibrils can accommodate liquids and media components as well as small

68   particles, thus supporting the formation of composites with several nano- and biocompatible

69   polymeric materials.

70   Several methods have been reported for the synthesis of composites of microbial

71   cellulose with other materials such as in situ, ex situ, and solvent dissolution and regeneration

72   methods.[1,2] However, these methods have several limitations such as the in situ method

73   encounters limitation due to the cytotoxic effects of bactericidal elements against microbial cells;

74   the ex situ method is confined to only nano-sized materials owing to the difficulty of penetrating

75   the well-arranged fibril network; and the solvent dissolution and regeneration method alters the

76   reticulate structure of microbial cellulose, and consequently, its physico-mechanical and

77   biological properties.[1,2,18]. Thus, the need was extensively felt to develop an alternative approach

78   for producing cellulose and preparing its composites with a wide range of materials for

79   multifarious applications. Recently, we have developed a cell-free system for production of bio-

80   cellulose that showed improved yield.[19] Moreover, the produced bio-cellulose exhibited

81   improved physico-mechanical properties.[20] The system was entirely comprised of enzymes and

82   not the microbial cells, and hence, can be utilized for the in situ preparation of composites of bio-

83   cellulose with a wide range of nanomaterials of any type and size.

84   The current study was aimed to develop nanocomposites of bio-cellulose with TiO_2

85   nanoparticles through an in situ strategy using a cell-free system. The synthesis mechanism of

86   nanocomposite by a cell-free system was described, and its structural features and antibacterial

87   activity against bacterial cells were investigated. This developed approach for the synthesis of

88   nanocomposite can be effectively extended to the synthesis of other composite materials of

89   diverse nature and a wide range of applications.

Materials and methods

90

Materials

91

92   The chemical reagents including titanium tetrachloride ($TiCl_4$), anhydrous benzyl alcohol

93   ($C_6H_5CH_2OH$), glucose ($C_6H_{12}O_6$), sodium hydroxide (NaOH), osmium tetroxide (OsO_4),

94   phosphate-buffered saline (PBS), glutaraldehyde [$CH_2(CH_2CHO)_2$], succinic acid ($C_4H_6O_4$),

95   acetic acid (CH_3COOH), and glass beads (425-600 µm) were purchased from Sigma-Aldrich (St.

96   Louis, MO, USA). Whatman® microfilter (0.45 µm) was purchased from GE Life Sciences

97   (Pittsburgh, PA, USA). Yeast extract and peptone were purchased from Becton, Dickinson and

98   Company (Le Pont de Claix, France). All the reagents were utilized in the experiments without

99   any additional processing.

Synthesis of TiO_2 nanoparticles and preparation of suspension

100

101   The TiO_2 nanoparticles were synthesized by slowly adding the $TiCl_4$ to benzyl alcohol in

102   a dropwise fashion as reported previously.[2,21] Briefly, 80 mL of benzyl alcohol was placed in a

103   pre-dried two-necked flask followed by the dropwise addition of 1 mL of $TiCl_4$ under nitrogen

104   flow. The mixture was heated to 80°C and stirred for 24 h. The resultant white suspension was

105   isolated and washed several times with distilled water and ethanol followed by calcination at

106   900°C for 1 h.

107   The TiO_2 nanoparticles suspension was prepared by sonication after suspending the

108   nanoparticles in distilled water with different concentrations of SDS solutions (0.5, 1, 2, and

109   5%). A suspension of TiO_2 nanoparticles prepared in distilled water was used as a reference. All

110   suspensions were sonicated at 25 min intervals until all the nanoparticles were in suspended

111   form. Thereafter, the suspensions were regularly observed for 15 days, after which their

112   absorbance was determined at 315 nm.

Microorganism and cell culture

114   *G. hansenii* PJK (KCTC 10505BP) was grown in a basal medium as described

115   previously.[1,19] Briefly, the basal medium was prepared by adding glucose 10 g/L, yeast extract

116   10 g/L, peptone 7 g/L, acetic acid 1.5 mL/L, and succinic acid 0.2 g/L to distilled water. The pH

117   of the medium was adjusted to 5.0 with 1.0 M NaOH. The prepared basal medium was sterilized

118   for 15 min at 15 psi and 121°C. A few colonies from the *G. hansenii* PJK culture plate were

119   inoculated into 100 mL of basal broth medium in a 250-mL Erlenmeyer flask and incubated for

120   24 h at 30°C under shaking conditions (150 rpm). Similarly, *E. coli* (KCCM 12119) was grown

121   on nutrient agar medium containing 3 g/L beef extract, 5 g/L peptone, and 15 g/L agar in

122   distilled water. The pH of the medium was adjusted to 7.0 with 1.0 M NaOH.

Development of the cell-free system

124   The cell-free system was developed using bead beating, as reported previously.[19,22-24]

125   Briefly, a freshly prepared 50 mL culture of *G. hansenii* PJK was taken in a Becton Dickinson

126   (BD) falcon tube and centrifuged at 3500 rpm for 15 min. The pellet was resuspended in 5 mL of

127   the supernatant to attain a 10× concentrated cell culture. The density of the culture rose to

128   2.6×10^7 cells/mL. Thereafter, equal volumes of the concentrated cell culture and sterile chilled

129   glass beads (425–600 µm) were put into a sterilized glass vial, and vortexed for 20 min to

130   rupture the bacterial cells. The samples were incubated on ice at regular intervals of 2.0 min

131   during beating to avoid thermal denaturation of the cellular proteins. The lysate was then

132   collected using a sterile syringe. The cell-free lysate was passed through a Whatman®

133   microfilter (0.45 μm) to remove cell debris, as described previously.[25] The protein concentration

134   of the cell-free lysate was determined by the Bradford assay and found to be 93.84 μg/mL.

135   **Synthesis of the bio-cellulose/TiO$_2$ nanocomposite**

136   Two parallel experiments were performed for the synthesis of bio-cellulose, and the bio-

137   cellulose/TiO$_2$ nanocomposite using the cell-free system. 1.0 mL of the suspension containing

138   0.0137 ± 0.0021 g of TiO$_2$ nanoparticles was added to the culture medium for the synthesis of

139   the nanocomposite. The synthesis was carried out in static culture for 3, 5, 10, and 15 days at

140   30°C and pH 5.0 using 10 g/L glucose. Bio-cellulose and bio-cellulose/TiO$_2$ nanocomposites

141   were harvested after 5 days (bio-cellulose/TiO$_2$-I), 10 days (bio-cellulose/TiO$_2$-II), and 15 days

142   (bio-cellulose/TiO$_2$-III) and washed several times with deionized distilled water until the pH

143   became neutral and all media components were removed. The samples were freeze-dried until

144   used for various analyses.

145   **Nanoparticles uptake analysis**

146   The initial amount of TiO$_2$ nanoparticles in the incubation mixture for nanocomposite

147   synthesis was determined using a standard curve generated using a UV-visible light spectra.[26]

148   The nanoparticles uptake during the in situ synthesis of the nanocomposite by the cell-free

149   system was determined through two methods described below:

150   **Dry-weight based analysis**

151   The weights of freeze-dried samples of bio-cellulose, bio-cellulose/TiO$_2$-I, bio-

152   cellulose/TiO$_2$-II, and bio-cellulose/TiO$_2$-III were determined. The difference of their dry-

153   weights gave the net weight of nanoparticles uptake by each nanocomposite during the in situ

154   synthesis by the cell-free system. Experiments were performed in triplicate, and the average

155   values were taken.

156 **Optical density method**

157   After harvesting the nanocomposites, the sample media from each vial was taken and

158 analyzed for the amount of TiO_2 nanoparticles by measuring its absorbance at 315 nm. The

159 difference of initial amount added to the incubation mixture and in the sample medium after

160 harvesting the nanocomposites gave the amount of TiO_2 nanoparticles that were impregnated

161 into the bio-cellulose during the in situ synthesis by the cell-free system. The experiment was

162 performed in triplicate, and the average values were taken.

163 **Characterization of the bio-cellulose/TiO$_2$ nanocomposite**

164   The in situ synthesis of the bio-cellulose/TiO_2 nanocomposite by the cell-free system was

165 confirmed through several techniques. FE-SEM of the bio-cellulose/TiO_2 nanocomposite was

166 performed using a Hitachi S-4800 and EDX-350 (Horiba) FE-SEM (Tokyo Japan). Briefly, the

167 samples were fixed onto a brass holder and coated with osmium tetroxide (OsO4) using a VD

168 HPC-ISW osmium coater (Tokyo Japan) prior to FE-SEM observation. Both surface morphology

169 and cross-sectional views of the samples were done. XRD patterns of both bio-cellulose and the

170 bio-cellulose/TiO_2 nanocomposite were recorded using an X-Ray diffractometer (X'Pert-APD

171 Philips, Netherlands) with an X-ray generator (3 KW) and anode (LFF Cu). The radiation was

172 CuK-α at 1.54 Å, the X-ray generator tension and current was 40 kV and 30 mA, respectively,

173 and the angle of scanning varied from 0 to 70°. The crystallinity indices of bio-cellulose and the

174 bio-cellulose/TiO_2 nanocomposite were determined from the peak area of the crystalline and

175 amorphous regions as reported previously.[15]

176 The crystallite size of both samples was calculated using the WHFM values through the Scherrer

177 equation given as follow:

178   $$L = \frac{K\lambda}{B\cos\theta}$$ (1)

179   where L represents the particle size; K is the Scherrer constant; λ is the wavelength of the X-ray;

180   θ is the diffraction angle of the peak; B represents the full width at half height of the peaks (in

181   radian). The crystallinities of both samples were calculated from the relative integrated area of

182   crystalline and amorphous peaks through the following equation:

183     $$Xc = \frac{Acr}{(Acr+Aam)} \times 100 \qquad\qquad (2)$$

184   where A_{cr} and A_{am} are the integrated area of the crystalline and amorphous phases,

185   respectively.[27]

186   Similarly, the FT-IR spectra of freeze-dried samples of bio-cellulose and the bio-

187   cellulose/TiO_2 nanocomposite were recorded by using a Perkin Elmer FTIR spectrophotometer

188   [Spectrum GX & Autoimage, USA, Spectral range: 4000–400 cm^{-1}; Beam splitter: Ge-coated on

189   KBr; Detector: DTGS; resolution: 0.25 cm^{-1} (step selectable)]. For analysis, the samples were

190   mixed with KBr (IR grade, Merck, Germany) pellets and processed further to obtain IR data that

191   was transferred to a PC to acquire the spectra as reported previously.[15]

192   **Thermal and mechanical properties of the bio-cellulose/TiO_2 nanocomposite**

193   The thermal properties of bio-cellulose and the bio-cellulose/TiO_2 nanocomposite were

194   determined through TGA analyses using a thermogravimetric/differential thermal analyzer

195   (Seiko Instruments Inc., Japan). A thermogram for TGA was obtained in the range of 25–800°C,

196   under nitrogen atmosphere with a temperature increase of 10°C min^{-1} as reported previously.[15]

197   Similarly,   the   tensile   properties   of   bio-cellulose   and   the   bio-cellulose/TiO_2

198   nanocomposite were measured using an Instron Universal Testing Machine (Model 4465, USA)

199   according to the procedure described by the American Society for Testing and Materials (ASTM

200   D 882). Briefly, two metal clamps were placed at either end of each 100 mm × 10 mm

201   rectangular strip of freeze-dried samples and then mounted on an Instron 4465 that measured

202   both elongation and maximum tensile load before fracture. The experiment was repeated several

203   times, and the average values were taken for each sample.

204   **Titanium (Ti^{4+}) release**

205   The amount of titanium (Ti^{4+}) released from the nanocomposite was determined by

206   immersing the freeze-dried bio-cellulose/TiO$_2$ nanocomposite (2 cm × 2 cm) in 5 mL of distilled

207   water for different lengths of time (0, 2, 4, 6, 8, and 10 days) at room temperature under static

208   conditions. After the respective period of time, the amount of Ti^{4+} released into the water was

209   quantified using an inductively coupled plasma spectrophotometer (ICP, Thermo Jarrell Ash

210   IRIS-AP).

211   **Antibacterial activity of the bio-cellulose/TiO$_2$ nanocomposite**

212   Antibacterial activities against *E. coli* of bio-cellulose and the bio-cellulose/TiO$_2$

213   nanocomposite were investigated through agar disc diffusion and optical density methods

214   described below:

215   **Agar disc diffusion method**

216   The antibacterial activity of bio-cellulose and bio-cellulose/TiO$_2$ nanocomposites was

217   measured on solid agar plates prepared using the *E. coli* growth media as reported previously.[1]

218   Briefly, freeze-dried samples of bio-cellulose, bio-cellulose/TiO$_2$-I, bio-cellulose/TiO$_2$-II, and

219   bio-cellulose/TiO$_2$-III were cut into disc shapes with a diameter 1.3 cm and sterilized at 121°C at

220   15 psi for 15 min. Next, a fresh pre-culture of *E. coli* was spread on the agar plate, and the discs

221   were placed on top and incubated at 37°C for 24 h. Finally, the inhibition zones were measured.

222   Herein, the disc prepared from bio-cellulose was used as a control.

223   **Optical density method**

224   The antibacterial activities of bio-cellulose, bio-cellulose/TiO$_2$-I, bio-cellulose/TiO$_2$-II,

225   and bio-cellulose/TiO$_2$-III were investigated through optical density method using *E. coli* growth

226   medium as reported previously.[1] Briefly, freeze-dried samples were sliced into small pieces and

227   sterilized at 121°C at 15 psi for 15 min. Next, 10 mL of growth medium for *E. coil* was added to

228   separate test tubes, followed by 0.02 g/mL of finely sliced solid bio-cellulose and bio-

229   cellulose/TiO$_2$ nanocomposites. The test tubes were then inoculated with 1 mL of fresh *E. coli*

230   culture and incubated in a shaking incubator at 37°C and 150 rpm for 24 h. During incubation,

231   the turbidity of the media at 610 nm was observed using a UV spectrophotometer (T60 U,

232   China).

233   **Statistical analysis**

234   The presented data are the mean values ± standard deviation (SD) of three independent

235   experiments. The results were analyzed by Student's t tests using the Statistical Package for the

236   Social Sciences (SPSS) software. *p* values ≤ 0.05 were considered statistically significant.

237   **Results and Discussion**

238   **Characterization of titanium dioxide nanoparticles and suspension**

239   The UV-visible spectrum of the TiO$_2$ nanoparticle suspension (Fig. 1A) was determined

240   between 150 to 700 nm that gave a central peak at 315 nm (Fig. 1B). This is caused by the

241   excitation of electrons from the valence band to the conduction band of titania. The sharp

242   absorption peak indicates a narrow particle size distribution, which is in agreement with previous

243   reports.[2,21] The XRD spectrum of TiO$_2$ nanoparticles further confirmed the UV spectrum results.

244   Various crystallinic peaks of TiO$_2$ nanoparticles are shown in Figure 1C, which confirms the

245   synthesis of anatase TiO$_2$ nanoparticles. The peaks at 2θ 25.23°, 36.95°, 37.71°, 38.56°, 48.06°,

246   53.80°, 55.07°, 62.75°, 68.71°, and 70.32° were assigned to the (101), (103), (004), (112), (200),

11

247 (105), (211), (118), (116), and (220) planes of anatase TiO_2, respectively, which is in agreement

248 with previous observations.[2,28] The FWHM values for all Miller indices ranged from 0.3°–0.4°

249 while the crystal size was in the range of 20-30 nm. The absence of extra peaks in the XRD

250 spectra confirmed the purity of the of TiO_2 nanoparticles.

251   A naked-eye observation of TiO_2 nanoparticles suspensions in both distilled water and

252 various concentrations of SDS solutions after sonication showed that the nanoparticles started

253 settling down with the passage of time (Fig. 1A). Nearly all TiO_2 nanoparticles suspended in

254 distilled water settled after 24 h. However, the settling rate was much slower for the

255 nanoparticles suspended in different concentrations of SDS solutions. It was observed that nearly

256 all of the nanoparticles suspended in the SDS solutions remained suspended for 15 days, which is

257 in agreement with previous observations.[29,30] These results show that the resuspension ability of

258 TiO_2 nanoparticles was extended by the addition of detergent during sonication. This improved

259 feature could be very useful during the in situ synthesis of a nanocomposite of bio-cellulose with

260 TiO_2 by a cell-free system.

261 **Synthesis of the bio-cellulose/TiO_2 nanocomposite**

262   Microbial cellulose production is an aerobic process where cellulose is produced at the

263 air-media interface as an assembly of reticulated crystalline ribbons and forms a gel-like

264 membrane.[15,31] Unlike microbial cellulose, bio-cellulose production can take place under

265 anaerobic conditions due to the involvement of enzymes in a cell-free system. It is produced in

266 the form of microfibrils that are uniformly distributed in the culture medium rather at the air-

267 medium interface.[19,20] In the current study, bio-cellulose/TiO_2 nanocomposites were synthesized

268 by an in situ strategy using a cell-free system. The nanocomposite was analyzed through FE-

269   SEM to confirm the impregnation of TiO_2 nanoparticles into the bio-cellulose matrix and its

270   synthesis mechanism during the in situ development by a cell-free system. A detailed description

271   suggesting the possible mechanism of impregnation of TiO_2 nanoparticles into the bio-cellulose

272   has been described in Figure 2.

273   Figure 2 shows the SEM micrographs of surface and cross section of bio-cellulose, bio-

274   cellulose/TiO_2-I, bio-cellulose/TiO_2-II, and bio-cellulose/TiO_2-III nanocomposites synthesized

275   after 5, 10, and 15 days, respectively by the cell-free system. It shows that the TiO_2 nanoparticles

276   were impregnated into the bio-cellulose matrix, confirming the successful synthesis of

277   nanocomposite through the in situ strategy. During nanocomposite synthesis, the suspended TiO_2

278   nanoparticles in the culture medium interact with the developing subfibrils from β-1,4-glucan

279   chains that form the micro and macro fibrils, bundles, and ribbons.[16,17] The nanoparticles are

280   encaged within the bio-cellulose matrix through hydrogen bonding.[15] The synthesis of bio-

281   cellulose/TiO_2-I showed that the TiO_2 nanoparticles were attached to the fibrils only and were

282   not impregnated into the matrix as shown in Figure 2(a). These observations were in agreement

283   with the cross sectional analysis of the bio-cellulose/TiO_2-I nanocomposite that displayed the

284   presence of TiO_2 nanoparticles towards the outer surface only and not in the interior of the bio-

285   cellulose matrix (Fig. 2b). Such arrangement of TiO_2 nanoparticles in the bio-cellulose matrix

286   could be attributed to the early phase of synthesis by the cell-free system that possessed a loosely

287   arranged matrix. The compactness of the bio-cellulose matrix increases with time as more fibrils

288   and pellicles are produced with the time and added to the pre-existing ones.[19,32,33] This resulted in

289   an increased density of TiO_2 nanoparticles within the matrix of bio-cellulose/TiO_2-II as shown in

290   Figure 2c. These observations were in agreement with the cross-sectional analysis of bio-

291   cellulose/TiO_2-II nanocomposite that displayed the presence of TiO_2 nanoparticles in the interior

292   of bio-cellulose matrix (Fig. 2d). The density of TiO_2 nanoparticles kept on increasing in the bio-

293   cellulose matrix with time, and a nanocomposite with uniform and deeply impregnated

294   nanoparticles was synthesized as shown by the surface (Fig. 2e) and cross-sectional analyses of

295   the bio-cellulose/TiO_2-III nanocomposite (Fig. 2f).

296   The potential application of a nanocomposite is highly dependent on the amount of

297   impregnated nanoparticles. The conventionally reported strategies of nanocomposite synthesis

298   such as in situ, ex situ, and solvent dissolution and regeneration approaches encounter the

299   limitation of inefficient nanoparticles uptake. This study attempted to overcome this limitation

300   through the development of an in situ strategy using a cell-free system. The nanoparticles uptake

301   during the in situ synthesis of nanocomposite by a cell-free system was determined through two

302   methods: dry-weight analysis and optical density method. The difference of initial nanoparticles

303   concentration added to the mixture and after harvesting the nanocomposite after the respective

304   time period gave the amount of nanoparticles impregnated into the bio-cellulose/TiO_2

305   nanocomposites. The detailed results are described below:

306   The dry-weight analyses of pure bio-cellulose and bio-cellulose/TiO_2 nanocomposite

307   produced under the same experimental conditions by a cell-free system were done to determine

308   the amount of TiO_2 nanoparticles impregnated into the nanocomposite. Table 1 shows that

309   0.0271 ± 0.0038 g, 0.0578 ± 0.0105 g, and 0.0832 ± 0.0108 g bio-cellulose was produced after 5,

310   10, and 15 days, respectively by the cell-free system. On the other hand, the dry-weights of bio-

311   cellulose/TiO_2-I, bio-cellulose/TiO_2-II, and bio-cellulose/TiO_2-III nanocomposites were found to

312   be 0.0281 ± 0.0042 g, 0.0604 ± 0.0123 g, and 0.0885 ± 0.0084 g, respectively. This indicates the

313   impregnation of 0.0010 g, 0.0026 g, and 0.0054 g corresponding to 3.55%, 4.30%, and 5.99% of

314   the total weights of bio-cellulose/TiO_2-I, bio-cellulose/TiO_2-II, and bio-cellulose/TiO_2-III

315   nanocomposites, respectively. These results show that the impregnation of TiO_2 nanoparticles

316   kept increasing with increased time, and 39.4% of the initially added TiO_2 nanoparticles (i.e.

317   0.0137 ± 0.0021 g) were successfully impregnated into the nanocomposite after 15 days. These

318   results are justified by the SEM micrographs that show a clear and increasing trend of

319   nanoparticles impregnation into the bio-cellulose matrix with increasing time (Fig. 2).

320   The results of the optical density method indicated a similar trend to that of dry-weight

321   analysis. Optical density analysis of sample medium after harvesting the bio-cellulose/TiO_2-I,

322   bio-cellulose/TiO_2-II, and bio-cellulose/TiO_2-III nanocomposites was carried out using a TiO_2

323   standard curve. The initial amount of TiO_2 nanoparticles in the culture medium was found to be

324   0.0137 ± 0.0021 g determined by the standard curve. The amounts of TiO_2 nanoparticles

325   impregnated into the nanocomposites, and non-impregnated nanoparticles in the culture medium

326   are given in Table 1. The optical density analysis of the culture medium shows that 0.0104 ±

327   0.0011 g, 0.0078 ± 0.0031 g, and 0.0055 ± 0.0022 g of nanoparticles were still present in the

328   culture medium after the synthesis of bio-cellulose/TiO_2-I, bio-cellulose/TiO_2-II, and bio-

329   cellulose/TiO_2-III nanocomposites, respectively. This indicates that 0.0008 g, 0.0034 g, and

330   0.0057 g of TiO_2 nanoparticles, corresponding to 5.83%, 24.81%, and 41.60% of the initially

331   added nanoparticles, were successfully taken up by the bio-cellulose/TiO_2-I, bio-cellulose/TiO_2-

332   II, and bio-cellulose/TiO_2-III nanocomposites, respectively. This is also justified by the SEM

333   micrographs   of   bio-cellulose/TiO_2-I,   bio-cellulose/TiO_2-II,   and   bio-cellulose/TiO_2-III

334   nanocomposites synthesized in situ by the cell-free system.

335   Table 1 shows a slight difference between the initially added nanoparticles and the sum

336   of impregnated and unattached nanoparticles in the culture medium. This difference could be

337   attributed to the amount of loosely bound nanoparticles that are removed during the washing of

338 nanocomposites. The amount of TiO_2 nanoparticles impregnated into the bio-cellulose matrix

339 determined through the above two different approaches were comparable. A significant

340 difference in the dry-weights of bio-cellulose and bio-cellulose/TiO_2 nanocomposites and optical

341 density values of culture media before and after the harvesting the nanocomposites showed that

342 TiO_2 nanoparticles were successfully impregnated into the bio-cellulose matrix. Further, the

343 content of impregnated nanoparticles kept on increasing with time and $40 \pm 1.6\%$ of the initially

344 added TiO_2 nanoparticles were successfully impregnated into the matrix after 15 days.

345 From the above results, it can be concluded that nanoparticles interact with the

346 microfibrils of bio-cellulose during the early phase of synthesis by a cell-free system. More

347 nanoparticles get impregnated with increasing time and are entrapped more towards the interior

348 of bio-cellulose matrix due to the addition of fibrils and pellicles. Several pellicles containing the

349 impregnated nanoparticles interact with each other and form the larger bio-cellulose sheet

350 containing a large number of impregnated TiO_2 nanoparticles (i.e. nanocomposite). The

351 thickness of nanocomposite increases in all directions when more pellicles containing the

352 impregnated nanoparticles are attached. This process continues until all of the substrate available

353 in the medium is consumed, and thus, a nanocomposite with a large number of impregnated

354 nanoparticles is formed. These observations suggest that the in situ synthesis approach using a

355 cell-free system ensures the uniform distribution of nanoparticles within the bio-cellulose matrix.

356 **Characterization of the bio-cellulose/TiO_2 nanocomposite**

357 The synthetic accuracy and structural features of the synthesized nanocomposites were

358 confirmed through FTIR and XRD analyses. The combined FTIR spectra of bio-cellulose and the

359   bio-cellulose/TiO_2 nanocomposite are shown in Figure 3A, indicating the positions of various

360   functional groups.

361   The FT-IR spectra of bio-cellulose contained basic peaks for all chemical groups in

362   cellulose and thereby confirmed the basic structure of pure cellulose. The spectra of bio-cellulose

363   showed characteristic peaks for OH stretching at 3,364 cm^{-1}, which are in agreement with

364   previous observations.[14,18,20] A broader peak for bio-cellulose indicated stronger OH bonding.[20]

365   Similarly, peaks were obtained for a CH stretching vibration at 2,924 cm^{-1} as reported

366   previously.[14,18,20] The presence of the CH group was further supported by the appearance of

367   several peaks corresponding to CH bending vibrations at 1450–1200 cm^{-1}.[13,20] In addition, two

368   characteristic peaks at 1,453 cm^{-1} and 1,396 cm^{-1} were observed.[20] The peaks due to C-O-C

369   stretching vibrations appeared at 1,060 cm^{-1}.[13,20,34] The FT-IR spectrum of bio-cellulose/TiO_2-III

370   nanocomposite contained additional small peaks at 621 cm^{-1}, 594 cm^{-1}, 549 cm^{-1}, and 412

371   cm^{-1}, which are in agreement with previous observations.[35] The presence of these characteristic

372   Ti-O peaks of titania confirms the successful synthesis of bio-cellulose/TiO_2-III nanocomposite

373   by a cell-free system through an in situ strategy. The peaks at 1000–1300 cm^{-1} for bio-

374   cellulose/TiO_2-III nanocomposite due to C–OH stretching (1060 cm^{-1}) and C–O–C bending

375   vibrations (1163 cm^{-1}), are weakened in comparison to the peaks in bio-cellulose because the

376   TiO_2 nanoparticles grow on the surface of bio-cellulose. These results are in agreement with

377   previous observation.[36]

378   Figure 3B shows the comparative XRD patterns of the extended linear scanning (10-70°)

379   of bio-cellulose and bio-cellulose/TiO_2-III nanocomposite. The XRD spectrum of bio-cellulose

380   showed two broad peaks at 2θ 11.78° and 20.32° arising from the (110-) and (110) crystallinic

381   planes, respectively, which represents the cellulose II structure.[20] The XRD pattern of bio-

382   cellulose/TiO$_2$-III nanocomposite showed the diffraction pattern of both bio-cellulose and TiO$_2$

383   nanoparticles that exhibit all characteristic peaks at 2θ 11.78°, 20.32°, 25.23°, 36.95°, 37.71°,

384   38.56°, 48.06°, 53.80°, 55.07°, 62.75°, 68.71°, and 70.32° arising from the (101), (103), (004),

385   (112), (200), (105), (211), (118), (116), and (220) planes of anatase TiO$_2$ nanoparticles.[2,28] The

386   slight decrease in the peak intensity of bio-cellulose in the bio-cellulose/TiO$_2$-III spectra could be

387   due to the TiO$_2$ content.[2]

388   The degree of crystallinity of bio-cellulose and bio-cellulose/TiO$_2$-III nanocomposite was

389   calculated from the relative integrated area of the crystalline and amorphous peaks (Eq. 2). The

390   ratio of crystalline to amorphous regions varies between samples and is dependent on the

391   cellulose type, microbial strain, medium constituents, and processing conditions.[37] The relative

392   crystallinity of bio-cellulose was 31.98%. This lower crystallinity of bio-cellulose was clearly

393   demonstrated by the absence of sharp crystallinic peaks in its XRD spectrum (Fig. 3B), and can

394   be attributed to the incomplete growth of crystallite during its synthesis by a cell-free system.[20]

395   The impregnation of TiO$_2$ nanoparticles did not significantly affect the crystallinity of bio-

396   cellulose, which was slightly reduced to 31.08%.[2] The crystallite size of bio-cellulose was

397   calculated through the Scherrer equation and is summarized in Table 2.

398   **Thermal and mechanical properties of the bio-cellulose/TiO$_2$ nanocomposite**

399   Besides various physico-mechanical and biological properties, the commercial

400   applications of cellulose are highly dependent on its thermal stability, especially at elevated

401   temperatures.[20,87,39] Further, highly thermostable inorganic materials, such as nanoparticles,

402   significantly increase the thermal degradation temperature of polymers.[1] Therefore, the thermal

403   behavior of the bio-cellulose/TiO_2-III nanocomposite was investigated using TGA and was

404   compared to that of bio-cellulose. The TGA thermograms of bio-cellulose and the bio-

405   cellulose/TiO_2 nanocomposite are shown in Figure 4A. The thermal degradation of bio-cellulose

406   takes place in three steps including dehydration, depolymerization, and decomposition of glucose

407   units, which finally results in charred residue.[40]

408   In the present study, both bio-cellulose and the bio-cellulose/TiO_2-III nanocomposite

409   displayed two major weight loss zones (Fig. 4A). In the first step, about 2-3% weight loss

410   occurred at a temperature range of 90–100°C in bio-cellulose. This weight loss in bio-cellulose

411   could be attributed to the loss of moisture content adsorbed on the surfaces and interlayer

412   coordinated water molecules.[41,42] The weight loss in the first step was lower for the bio-

413   cellulose/TiO_2 nanocomposite, indicating that the sample had a lower water content.[1] Negligible

414   weight loss was observed as the temperature was increased to 290°C and 310°C for bio-cellulose

415   and the bio-cellulose/TiO_2 nanocomposite, respectively. The second phase revealed a sharp

416   weight loss due to the degradation of the main cellulose skeleton in both samples.[15,20,41] The

417   onset temperatures of bio-cellulose and the bio-cellulose/TiO_2 nanocomposite were 298°C and

418   333°C, respectively. The improved thermal stability of nanocomposite could be attributed to the

419   impregnated TiO_2 nanoparticles. During this phase, the weight loss in bio-cellulose was 84%. In

420   contrast, a lower weight loss was recorded in the bio-cellulose/TiO_2 nanocomposite (68%).

421   Similarly, the endset temperatures of bio-cellulose and bio-cellulose/TiO2 nanocomposite were

422   346°C and 411°C, respectively. The overall results indicate that the thermal stability of bio-

423   cellulose/TiO_2 nanocomposite was higher than bio-cellulose. Figure 4A also indicates that there

424   was no further decomposition of TiO_2 nanoparticles after bio-cellulose degradation. Inorganic

425   materials are thermally stable and most degrade above 600°C.[1] The nanoparticles impregnated

19

426 into polymers, such as cellulose, offer a barrier for the main skeleton by absorbing heat, which

427 ultimately results in shifting the degradation process towards higher temperature and reduced

428 weight loss.

429 Figure 4B shows the mechanical properties of bio-cellulose and bio-cellulose/TiO_2-III

430 nanocomposite. The maximum tensile strength value at the breaking point for bio-cellulose was

431 recorded to be 17.54 MPa. This high value could be attributed to the thick, compact, and well-

432 arranged fibrils of bio-cellulose.[20] Such compact and uniform arrangement of fibrils in bio-

433 cellulose could give a uniform response to applied force, and thus, result in improved tensile

434 strength.[15,37] The tensile strength for bio-cellulose/TiO_2-III nanocomposite was increased to

435 20.98 MPa. Similar increases in tensile properties of polymer-nanoclay and polymer-

436 nanoparticles have previously been reported.[1,43,44] The Young's modulus for the bio-

437 cellulose/TiO_2-III nanocomposite was significantly increased to 0.97 GPa comparing to 0.38

438 GPa of bio-cellulose. These results demonstrate that the impregnation of TiO_2 nanoparticles

439 exerts a positive effect on the mechanical properties of bio-cellulose. It has been reported that the

440 binding potential of nanoparticles to the polymer surface is readily affected by the physical

441 phenomenon caused by rough surfaces and chemical interactions by hydrogen bonding and Van

442 der Waals forces.[1,45] The binding of TiO_2 and ZnO nanoparticles with microbial cellulose with

443 OH moieties have already been reported.[1,2] The TiO_2 nanoparticles attached to bio-cellulose

444 improves its overall toughness and restricts its mobility, ultimately resulting in the improved

445 mechanical strength of the nanocomposite.[1,46] The average strain of bio-cellulose and the bio-

446 cellulose/TiO_2-III nanocomposite was recorded to be 3.29 and 2.74%, respectively. The low

447 strain of bio-cellulose could be attributed to the closely packed fibrils that cause the chains to be

448 almost immobile and results in a very low level of elasticity.[20] The strain of the nanocomposite

20

449　was significantly decreased upon the incorporation of TiO_2 nanoparticles into bio-cellulose.

450　Several studies have reported a decrease in elasticity of composite material that can be attributed

451　to the incorporation of nanoparticles into the main cellulose skeleton.[1,15,46] The binding

452　interaction between the TiO_2 nanoparticles causes rigidity and restricts the mobility of bio-

453　cellulose microfibrils, thus, resulting in decreased strain.

454　**Antibacterial properties of the bio-cellulose/TiO_2 nanocomposite**

455　　　Lack of antibacterial properties in microbial and bio-cellulose is one of the main motives

456　behind the synthesis of composites with bactericidal materials. To date, several nanocomposites

457　of microbial cellulose have been reported to have excellent antibacterial and antifungal

458　activities.[1,2,47] Khan et al. have demonstrated a detailed mechanism of action of nanoparticles and

459　nanocomposite against *E. coli*.[2] In general, nanocomposites show their bactericidal activity

460　through oxidative stress, generation of reactive oxygen species such as H_2O_2, O_2^-, O_2* and $OH^·$,

461　membrane stress, or the release of ions.[2] Oxidative stress is a key antibacterial mechanism of

462　nanomaterials caused by several factors including the generation of reactive oxygen species

463　which induces mitochondrial membrane permeability and damages the cellular respiratory chain.

464　ROS can also lead to the generation of free radicals either through interaction with cellular

465　components or via activation of NADPH-oxidase enzyme. [48] Membrane stress caused by the

466　direct contact with nanomaterials is another possible effect on bacterial cell viability.[49] This

467　direct contact of nanomaterials with bacterial cell damages the peptidoglycans which results in

468　altered morphology of bacterial cell. TiO_2 nanoparticles and bio-cellulose/TiO_2 nanocomposite

469　produces highly reactive species which decompose the cell's outer membrane consisting of

470　lipopolysaccharide (LPS) and peptidoglycan as reported previously.[2] The phospholipid layer is

471　also damaged by the free radicals such as O_2^- and $OH^·$.[2]

472   The antibacterial activity against *E. coli* of bio-cellulose and the bio-cellulose/TiO$_2$

473   nanocomposites developed by a cell-free system was investigated using the agar disc diffusion

474   and optical density methods. The results of are shown in Figures 5A and 5B. During the disc

475   diffusion method, the impregnated nanoparticles immediately begin to diffuse outwards from the

476   nanocomposite disc. The released nanoparticles create a gradient in the agar such that the highest

477   concentration is found in the vicinity of the disc while decreasing the concentrations further

478   away from the disc. For bio-cellulose, the disc did not produce any inhibition zone (Fig. 5A),

479   indicating that it does not possess any bactericidal activity, which is in agreement with previous

480   studies.[1,14,50] On the other hand, clear inhibition zones or 'areas of no growth' were produced by

481   the bio-cellulose/TiO$_2$-I, bio-cellulose/TiO$_2$-II, bio-cellulose/TiO$_2$-III nanocomposites discs after

482   an overnight incubation. Precisely, a maximum of 3.7 cm, 2.5 cm, and 2.1 cm zones of inhibition

483   were produced by the bio-cellulose/TiO$_2$-I, bio-cellulose/TiO$_2$-II, bio-cellulose/TiO$_2$-III

484   nanocomposites, respectively. The results obtained with disc diffusion method were in

485   agreement with those of the optical density method that showed similar trends of antibacterial

486   activity. The curves for optical density values versus culture time for bio-cellulose and bio-

487   cellulose/TiO$_2$ nanocomposites are shown in Figure 5B. The results indicate that bio-cellulose

488   did not show any antibacterial activity and, in fact, the *E. coli* growth was higher than the

489   control, which is in agreement with previous reports.[2,51] In contrast, the nanocomposites showed

490   considerable antibacterial activity against *E. coli*, which was higher for bio-cellulose/TiO$_2$-III

491   compared to the bio-cellulose/TiO$_2$-II and bio-cellulose/TiO$_2$-I nanocomposites. This indicates

492   that the bactericidal effect of the bio-cellulose/TiO$_2$ nanocomposite is dependent on TiO$_2$

493   concentration and release rat[52,53] These observations are in agreement with the SEM micrographs

494   of the nanocomposites (Fig. 2). This can be further explained by the fact that with increasing

495   time the bio-cellulose fibrils become more compact and hold the nanoparticles more firmly,

496   which allows for the slow release of nanoparticles that show bactericidal activity over a

497   prolonged time. Consequently, this will improve the potential of application of bio-

498   cellulose/TiO_2 nanocomposites in the biomedical field.

499   The release behavior of ions or nanoparticles indicates the strength of their interaction

500   with the polymer matrix and their toxicological level.[1,2] Further, the constant and controlled

501   release of nanoparticles is necessary for biomedical and other applications, which may otherwise

502   cause hazardous effect if high concentrations are released or if a release occurs in an

503   uncontrolled fashion. A nanocomposite of cellulose with TiO_2 nanoparticles shows its

504   antibacterial activity due to the release of Ti^{4+}.[2] Therefore, the Ti^{4+} release behavior from bio-

505   cellulose/TiO_2-III nanocomposite was determined.

506   In the current study, the amount of Ti^{+4} released from the bio-cellulose/TiO_2-III

507   nanocomposite in water was determined using the ICP method. The nanocomposite showed a

508   very low level of ion release throughout the entire observation period. Precisely, the ions release

509   level reached to only 0.1123% of the initially impregnated nanoparticles in the nanocomposite

510   after 10 days of incubation in water under static conditions at room temperature (Table 3).

511   Conversely, the nanocomposite retained 99.98% of nanoparticles impregnated after 10 days of

512   incubation. This slow release of ions indicates the strong interaction of Ti^{+4} with bio-cellulose

513   fibers at both the surface and inner matrix as shown by the highly compact fibril arrangement in

514   the nanocomposite (Fig. 2).

515   **Comparative analysis of the nanocomposites synthesized through a cell-free system,**

516   **microbial cell system, and regeneration method**

517   To date, nanocomposites of microbial cellulose with TiO_2 nanoparticles have been

518 synthesized by various methods such as ex situ[36,54-56] and regeneration methods.[2] However, these

519 nanocomposites have several limitations including limited impregnation of nanoparticles into the

520 cellulose matrix, nanoparticle release, and variable distribution of nanoparticles.[36, 54-56] Further,

521 these nanocomposites have limited thermal and mechanical stability and low antibacterial

522 activity.[36,54] In the current study, we have developed a bio-cellulose/TiO_2 nanocomposite through

523 an in situ strategy using a cell-free system, which avoids the cytotoxic effect of TiO_2

524 nanoparticles on cells.[2]

525   Bio-cellulose synthesized by a cell-free system possesses a more compact and well-

526 distributed fibril arrangement[20] that favored the effective uptake of TiO_2 nanoparticles (Table 1).

527 Further, the TiO_2 nanoparticles were impregnated into the bio-cellulose matrix (Fig. 2) and

528 remained firmly attached to the fibers as shown by the slow release of Ti^{4+} from the synthesized

529 bio-cellulose/TiO_2-III nanocomposite (Table 3). On the other hand, the TiO_2 nanoparticles are

530 mostly attached to the bacterial cellulose (BC) surface in the ex situ method and a major portion

531 are released during the washing (e.g. with sodium carbonate solution) of the BC/TiO_2

532 nanocomposite.[52] Further, the in situ synthesis of nanocomposite by the cell-free system favored

533 the uniform distribution of TiO_2 nanoparticles due to the continuous synthesis of cellulose fibers

534 and their interaction with TiO_2 nanoparticles as shown by the FE-SEM micrographs (Fig. 2). In

535 contrast, the formation of agglomerates on the surface of a composite is a common phenomenon

536 during the ex situ synthesis of BC composites with TiO_2 or other nanomaterials.[52] The bio-

537 cellulose/TiO_2 nanocomposite synthesized by the cell-free system showed better thermal

538 properties as shown by the thermogravimetric analysis (Fig. 4A). The degradation temperature of

539 bio-cellulose/TiO_2 nanocomposite synthesized by the cell-free system was found to be 414°C

540   compared to 280-300°C for BC/TiO$_2$ nanocomposites as reported in previous studies.[36,54] On the

541   other hand, regeneration method of composite synthesis alters the reticulate structure of

542   microbial cellulose and ultimately its physico-mechanical properties.[1,2] Furthermore, the bio-

543   cellulose/TiO$_2$ nanocomposite synthesized by the cell-free system displayed better antibacterial

544   activity compared to RBC/TiO$_2$ nanocomposite created by the regeneration method.[2] This could

545   be due to the fact that uniformly distributed TiO$_2$ nanoparticles in the bio-cellulose/TiO$_2$

546   nanocomposite synthesized by the cell-free system are slowly and uniformly released and

547   showed bactericidal activity against *E. coli* for a prolonged time (Fig. 5B).

548   From the above discussion, it can be concluded that a cell-free system can offer several

549   advantages compared to microbial cell system in composite syntheses, such as in situ synthesis

550   of composites with a wide range of bactericidal elements, better uptake and uniform distribution

551   of nanoparticles, and cost effectiveness due to a better yield of bio-cellulose. Similarly, the

552   thicker, compact, and well-distributed fibers in bio-cellulose could favor the synthesis of a

553   composite with better physico-mechanical, antibacterial, and biological properties.

Conclusions

555   A bio-cellulose/TiO$_2$ nanocomposite was successfully developed through an in situ

556   approach using a cell-free system. The cell-free system developed from a single cell line through

557   a low-cost and simple approach bypassed the limitation of the nanoparticles' bactericidal effect

558   on the microbial cells that are used for in situ synthesis of nanocomposites. The nanocomposite

559   that was synthesized by the cell-free system showed improved thermal, mechanical, and

560   antibacterial properties compared to bio-cellulose. This could be an important aspect when

561   choosing a synthesis method (in situ synthesis by the cell-free system). The current synthesis

562   approach will provide a foundation for the future development of a broad range of composite

563   materials of biopolymers with bactericidal elements for various biomedical and other useful

564   applications.

Acknowledgements

570

References

571

572　1　M. Ul-Islam, W. A. Khattak, M. W. Ullah, S. Khan and J. K. Park, *Cellulose*, 2014, **21**, 433–

573　　　447.

574　2　S. Khan, M. Ul-Islam, W. A. Khattak, M. W. Ullah and J. K. Park, *Cellulose*, 2015, **22**, 565–

575　　　579.

576　3　T. Hanemann and D. V. Szabo, *Materials*, 2010, **3**, 3468–3517.

577　4　A. Aravamudhan, D. M. Ramos, J. Nip, M. D. Harmon, R. James, M. Deng, C. T. Laurencin,

578　　　X. Yu and S. G. Kumbar, *J. Biomed. Nanotechnol.*, 2013, **9**, 719–731.

579　5　M. Fiayyaz, K. M. Zia, M. Zuber, T. Jamil, M. K. Khosa and M. A. Jama, *Korean. J. Chem.*

580　　　*Eng.*, 2014, **31**, 644–649.

581　6　H. Zhang, Y. Shan and L. Dong, *J. Biomed. Nanotechnol.*, 2014, **10**, 1450–1457.

582　7　C. Seo and H. W. Lee, A. Suresh, J. W. Yang, J. K. Jung and Y. C. Kim, *Korean. J. Chem.*

583　　　*Eng.*, 2014, **31**, 1433-1437.

584　8　M. Shoda and Y. Sugano, *Biotechnol. Bioproc. E.*, 2005, **10**, 1-8.

585　9　W. Czaja, A. Krystynowicz, S. Bielecki and R. M. Brown, *Biomaterials*, 2006, **27**, 145–151.

586　10　K. Mahmoudi, K. Hosni, N. Hamdi and E. Srasra, *Korean. J. Chem. Eng.*, 2015, **32**, 274-283.

587　11　C. Wu and Y. K. Lia, *J. Mol. Catal. B: Enzym.*, 2008, **54**, 103–108.

588　12　H. X. Li, S. J. Kim, Y. W. Lee, C. D. Kee and I. K. Oh, *Korean. J. Chem. Eng.*, 2011, **28**,

589　　　2306–2311.

590　13　M. Ul-Islam, N. Shah, J. H. Ha and J. K. Park, *Korean. J. Chem. Eng.*, 2011, **28**, 1736–1743.

591　14　M. Ul-Islam, J. H. Ha, T. Khan and J. K. Park, *Carbohydr. Polym.*, 2013, **92**, 360–366.

592　15　M. Ul-Islam, T. Khan and J. K. Park, *Carbohydr. Polym.*, 2012, **88**, 596–603.

593　16　Y. Dahman, *J. Nanosci. Nanotechnol.*, 2009, **9**, 5105–5122.

594 17 A. Meftahi, R. Khajavi, A. Rashidi, M. Sattari, M. E. Yazdanshenas and M. Torabi,

595   *Cellulose*, 2010, **17**, 199–204.

596 18 M. Ul-Islam, W. A. Khattak, M. Kang, S. M. Kim, T. Khan and J. K. Park, *Cellulose*, 2013,

597   **20**, 253–263.

598 19 M. W. Ullah, M. Ul-Islam, S. Khan, Y. Kim and J. K. Park, *Carbohydr. Polym.*, 2015, **132**,

599   286–294.

600 20 M. W. Ullah, M. Ul-Islam, S. Khan, Y. Kim and J. K. Park, *Carbohydr. Polym.*, 2016, **136**,

601   908–916.

602 21 M. Niederberger, M. H. Bartl and G. D. Stucky, *Chem. Mat.*, 2002, **14**, 4364–4370.

603 22 M. W. Ullah, W. A. Khattak, M. Ul-Islam, S. Khan and J. K. Park, *Biochem. Eng. J.*, 2014,

604   **91**, 110-119.

605 23 M. W. Ullah, W. A. Khattak, M. Ul-Islam, S. Khan and J. K. Park, *Biotechnol. Bioprocess*

606   *Eng.*, 2015, **20**, 561-575.

607 24 Y. Jeon, J. Y. Yi and D. H. Park, *Korean. J. Chem. Eng.*, 2014, **31**, 475–484.

608 25 W. A. Khattak, M. Ul-Islam, M. W. Ullah, B. Yu, S. Khan and J. K. Park, *Process Biochem.*,

609   2014, **49**, 357–364.

610 26 D. Paramelle, A. Sadovoy, S. Gorelik, P. Free, J. Hobleya and D. G. Fernig. *Analyst*, 2014,

611   **139**, 4855–4861.

612 27 B. Focher, M. T. Palma, M. Canetti, G. Torri, C. Cosentino, G. Gastaldi, *Ind Crop Prod.*,

613   2001, **13**, 193–208.

614 28 L. Zhao, H. Wang, K. Huo, L. Cui, W. Zhang, H. Ni, Y. Zhang, Z. Wu and P. K. Chu,

615   *Biomaterials*, 2011, **32**, 5706–5716.

616   29 R. Chadha, R. Sharma, N. Maiti, A. Ballal and S. Kapoor, *Spectrochim. Acta, Part A.*, 2015,

617   **150**, 664–670.

618   30 E. Bae, H. J. Park, J. Park, J. Yoon, Y. Kim, K. Choi and J. Yi, *Bull. Korean Chem. Soc.*,

619   2011, **32**, 613-619.

620   31 R.   Mormino   and   H.   Bungay,   *Appl.   Microbiol.   Biotechnol.*,   2003,

621   **62**, 503–506.

622   32 S. Kaewnopparat, K, Sansernluk and D. Faroongsarng, *AAPS Pharm. Sci. Tech.*, 2008, **9**,

623   701–707.

624   33 W. Tang, S. Jia, Y. Jia and H. Yang, *World J. Microbiol. Biotechnol.*, 2010, **26**, 125–131.

625   34 N. Shah, J. H. Ha and J. K. Park, *Biotechnol. Bioprocess Eng.*, 2010, **15**, 110–118.

626   35 M. Hema, A. Y. Arasi, P. Tamilselvi and R. Anbarasan, *Chem. Sci. Trans.*, 2013, **2**, 239-245.

627   36 D. Sun, J. Yang and X. Wang, *Nanoscale*, 2010, **2**, 287–292.

628   37 O. Shezad, S. Khan, T. Khan and J. K. Park, *Carbohydr. Polym.*, 2010, **82**, 173–180.

629   38 M. W. Ullah, W. A. Khattak, M. Ul-Islam, S. Khan and J. K. Park, *Biochem. Eng. J.*, 2016,

630   **105**, 391-405.

631   39 Y. S. Lin and A. J. Burggraaf, *J. Am. Ceram. Soc.*, 1991, **74**, 219–224.

632   40 J. George, K. V. Ramana, A. S. Bawa and S. Siddaramaiah, *Int. J. Biol. Macromol.*, 2011, **48**,

633   50–57.

634   41 M. Darder, M. Colilla and E. Ruiz-Hitzky, *Chem. Mater.*, 2003, **15**, 3774–3780.

635   42 T. Khan and J. K. Park, *Carbohydr. Polym.*, 2008, **73**, 438–445.

636   43 H. Liu, D. Chaudhary, S. Yusa and M. O. Tade, *Carbohydr. Polym.*, 2010, **83**, 1591–1597.

637   44 S. T. Olalekan, S. A. Muyibi, Q. H. Shah, M. F. Alkhatib F. Yusof and I. Y. Qudsie, *Energy*

638   *Res*. J., 2010, **1**, 68–72.

639   45 D. Batch, J. L. Andres, J. E. Winter, H. B. Schlegel, J. M. Ball and J. W. Holobka, *J.*

640   *Adhesion. Sci. Technol.*, 1994, **8**, 249–259.

641   46 R. Velmurugan and T. P. Mohan, *J. Reinf. Plast. Compos.*, 2009, **28**, 17–37.

642   47 H. Chen, S. B. Lin, C. P. Hsu and L. C. Chen, *Cellulose*, 2013, **20**, 1967–1977.

643   48 T. Xia, M. Kovochich, M. Liong, L. Madler, B. Gilbert, H. Shi, J. I. Yeh, J. I. Zink and A. E.

644   Nel. *ACS Nano*, 2008, **2**, 2121–2134.

645   49 X. Jiang, L. Yang, P. Liu, X. Li and J. Shen. *Colloids Surf B*, 2010, **79**, 69–74.

646   50 W. L. Hu, S. Chen, X. Li, S. Shi, W. Shen, X. Zhang and H. Wang, *Mat. Sci. Eng. C. Bio. S.*,

647   2009, **29**, 1216–1219.

648   51 T. Maneerung, S. Tokura and R. Rujiravanit, *Carbohydr. Polym.*, 2008, **72**, 43–51.

649   52 Z. Emami-Karvani and P. Chehrazi, *Afr. J. Microbiol. Res.*, 2011, **5**, 1368–1373.

650   53 G. Applerot, A. Lipovsky, R. Dror, N. Perkas, Y. Nitzan, R. Lubart and A. Gedanken, *Adv.*

651   *Funct. Mater.*, 2009, **19**, 842–852.

652   54 J. Gutierrez, A. Tercjak, I. Algar, A. Retegi and I. Mondragon, *J. Colloid Interface Sci.*,

653   2012, **377**, 88–93.

654   55 A. Daoud, J. H. Xin and Y. H. Zhang, *Surf. Sci.*, 2005, **599**, 69–75.

655   56 X. Zhang, W. Chen, Z. Lin, J. Yao and S. Tan, *Synth. React. Inorg., Met.-Org., Nano-Met.*

656   *Chem.*, 2011, **41**, 997–1004.

657   **Table 1** Illustration of TiO_2 uptake during the in situ synthesis of bio-cellulose/TiO_2 nanocomposite by cell-free system. The initial

658   amount of TiO_2 added to the culture medium was 0.0137 ± 0.0021 g and the synthesis was carried out at 30°C and pH 5.0 under static

659   condition.

Nanocomposite	Experiment I (Dry-weight method)			Experiment II (Optical density method)	
	Dry weight (g)		TiO_2 up taken in	Amount of TiO_2 in	TiO_2 up taken in
	Bio-cellulose	Bio-cellulose/TiO_2	Bio-cellulose/TiO_2 (g)	culture medium (g)	Bio-cellulose/TiO_2 (g)
Bio-cellulose/TiO_2-I	0.0271 ± 0.0038	0.0281 ± 0.0042	0.0010	0.0104 ± 0.0011	0.0008
Bio-cellulose/TiO_2-II	0.0578 ± 0.0105	0.0604 ± 0.0123	0.0026	0.0078 ± 0.0031	0.0034
Bio-cellulose/TiO_2-III	0.0832 ± 0.0108	0.0885 ± 0.0084	0.0054	0.0055 ± 0.0022	0.0057

660

661   **Table 2** Illustration of comparative *d*-spacing, crystallinic planes, FWHM values, crystallite size,

662   and crystallinity index of bio-cellulose.

Sample	*d*-spacing (Å)	Crystallinic planes	FWHM	Crystallite sizes (Å)	Crystallinity index (%)
Bio-cellulose	6.1001	(1-10)	1.611	47	31.98
	3.8932	(110)	1.428	555	

663

664

665   **Table 3** Illustration of Ti^{4+} release from bio-cellulose/TiO_2 nanocomposite after different length

666   of time incubated at room temperature under static conditions.

Days	Initial amount of NPs in nanocomposite (g)	Amount of NPs released from nanocomposite (g)	%	Amount of NPs retained in nanocomposite (g)	%
0	0.0054	0	0.0000	0.005400	100
2	0.0054	9.53×10^{-7}	0.0177	0.005399	99.982335
4	0.0054	3.15×10^{-6}	0.0585	0.005397	99.941548
6	0.0054	4.55×10^{-6}	0.0843	0.005395	99.915652
8	0.0054	5.84×10^{-6}	0.1083	0.005394	99.891698
10	0.0054	6.063×10^{-6}	0.1123	0.005394	99.887721

667

668 **Figure legends**

669 **Graphical abstract:** In situ synthesis of bio-cellulose/TiO$_2$ nanocomposite possessing high

670 thermo-mechanical and antibacterial properties and showing uniform distribution and slow

671 release of nanoparticles.

672 **Fig. 1.** Illustration of **(A)** preparation of a TiO$_2$ nanoparticles suspension in different

673 concentrations of SDS (0.5, 1, 2, and 5%) through sonication, and naked eye observation after (I)

674 0 days (reference), (II) 5 days, (III) 10 days, and (IV) 15 days, **(B)** the UV-Visible spectrum of

675 TiO$_2$ nanoparticles, and **(C)** the X-ray diffraction pattern of TiO$_2$ nanoparticles.

676 **Fig. 2** FE-SEM analysis of (a) the surface and (b) cross-section of bio-cellulose/TiO$_2$-I, (c) the

677 surface and (d) cross section of bio-cellulose/TiO$_2$-II, and (e) the surface and (f) cross section of

678 bio-cellulose/TiO$_2$-III nanocomposites.

679 **Fig. 3A.** Fourier transform-infrared spectral analysis of bio-cellulose and the bio-cellulose/TiO$_2$

680 nanocomposite produced under static conditions at 30°C and pH 5.0.

681 **Fig. 3B.** The X-ray diffraction patterns of bio-cellulose and the bio-cellulose/TiO$_2$

682 nanocomposite produced under static conditions at 30°C and pH 5.0.

683 **Fig. 4A.** Thermal gravimetric analysis curves of bio-cellulose and the bio-cellulose/TiO$_2$

684 nanocomposite produced under static conditions at 30°C and pH 5.0.

685 **Fig. 4B.** The mechanical properties of bio-cellulose and the bio-cellulose/TiO$_2$ nanocomposite

686 produced under static conditions at 30°C and pH 5.0.

687   **Fig. 5A.** Evaluation of antibacterial activities against *E. coli* of (I) bio-cellulose, (II) bio-

688   cellulose/TiO_2-I, (III) bio-cellulose/TiO_2-II, and (IV) bio-cellulose/TiO_2-III nanocomposites as

689   determined by the disc diffusion method.

690   **Fig. 5B.** Illustration of antibacterial activities against *E. coli* of bio-cellulose, bio-cellulose/TiO_2-

691   I, bio-cellulose/TiO_2-II, and bio-cellulose/TiO_2-III nanocomposites as determined by the optical

692   density method. Data are the mean ± SD of three independent experiments. Significance was

693   indicated by *$p \leq 0.05$ relative to the control.
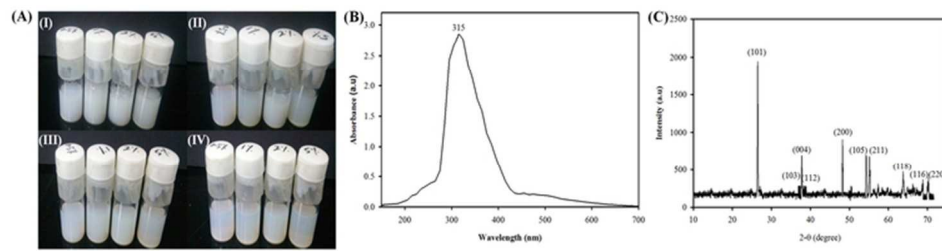
Ullah et al., Fig. 1

67x25mm (300 x 300 DPI)
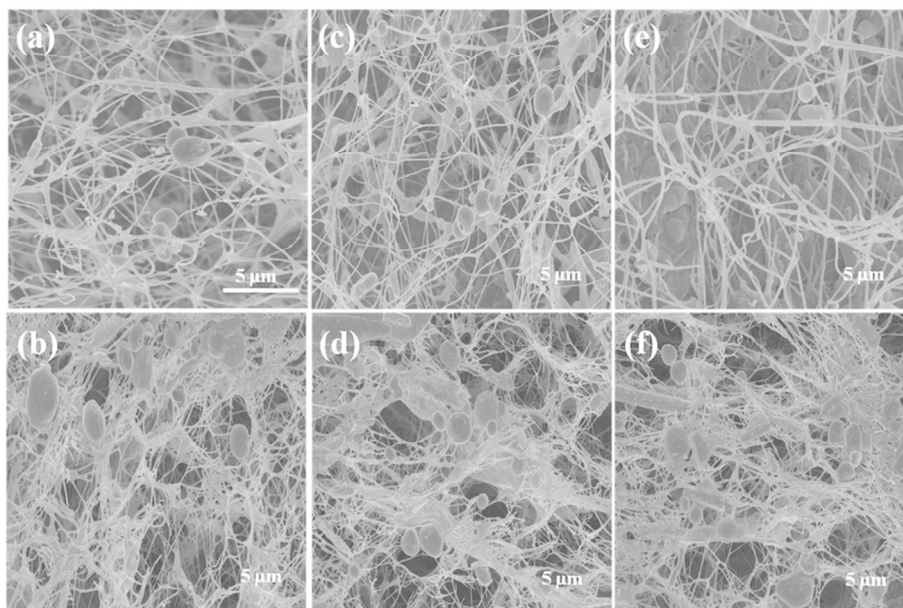
Ullah et al., Fig. 2

98x75mm (300 x 300 DPI)
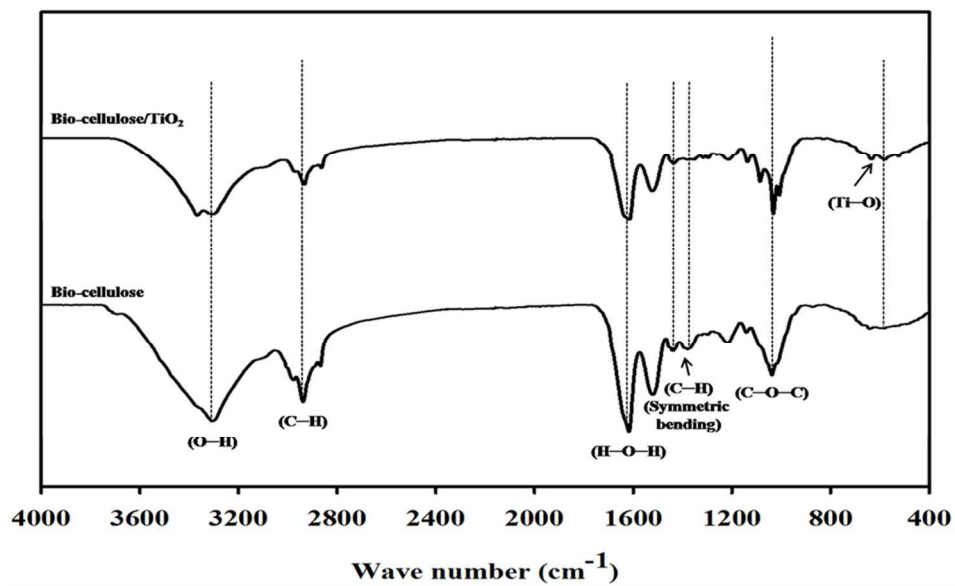
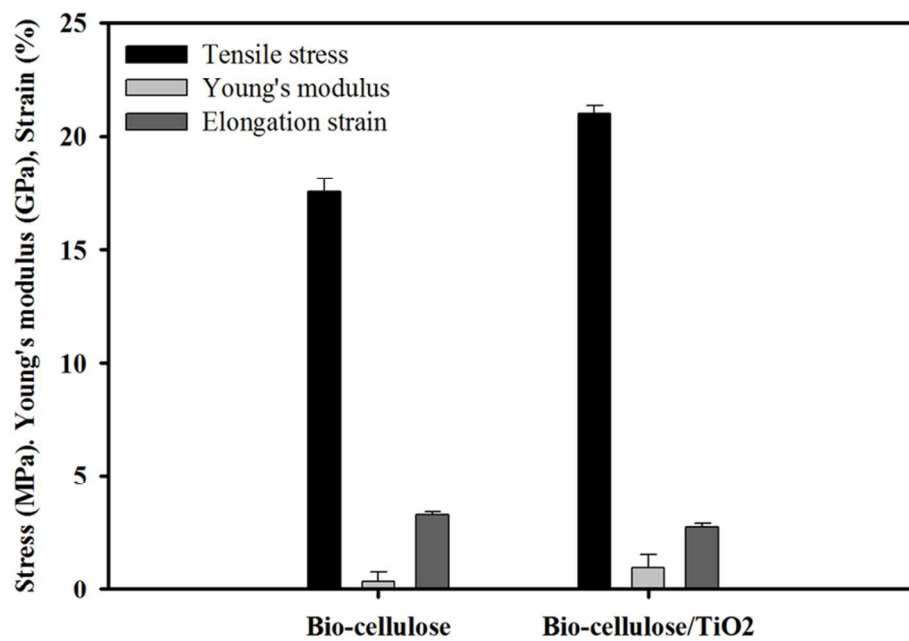Ullah et al., Fig. 3A

95x71mm (300 x 300 DPI)
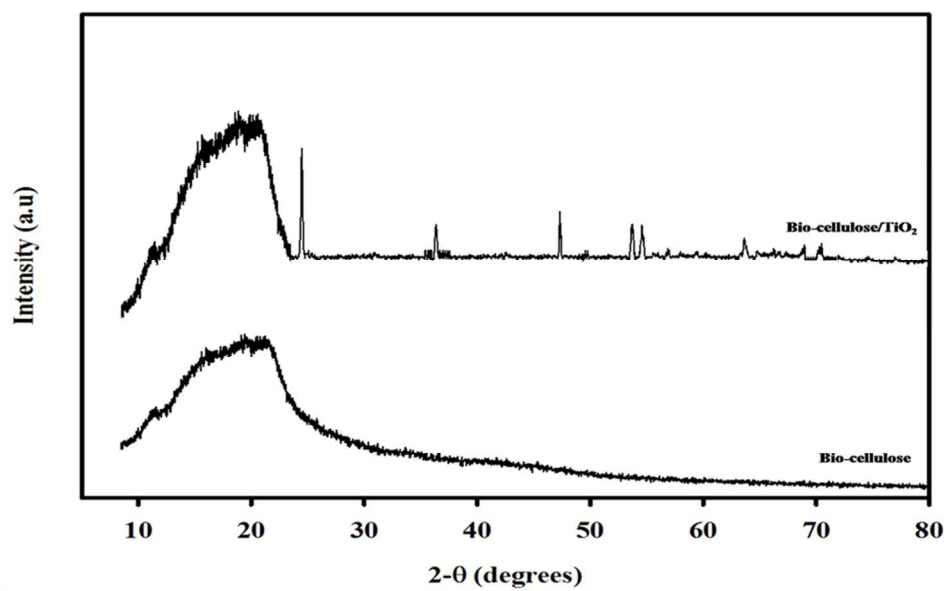
Ullah et al., Fig. 3B
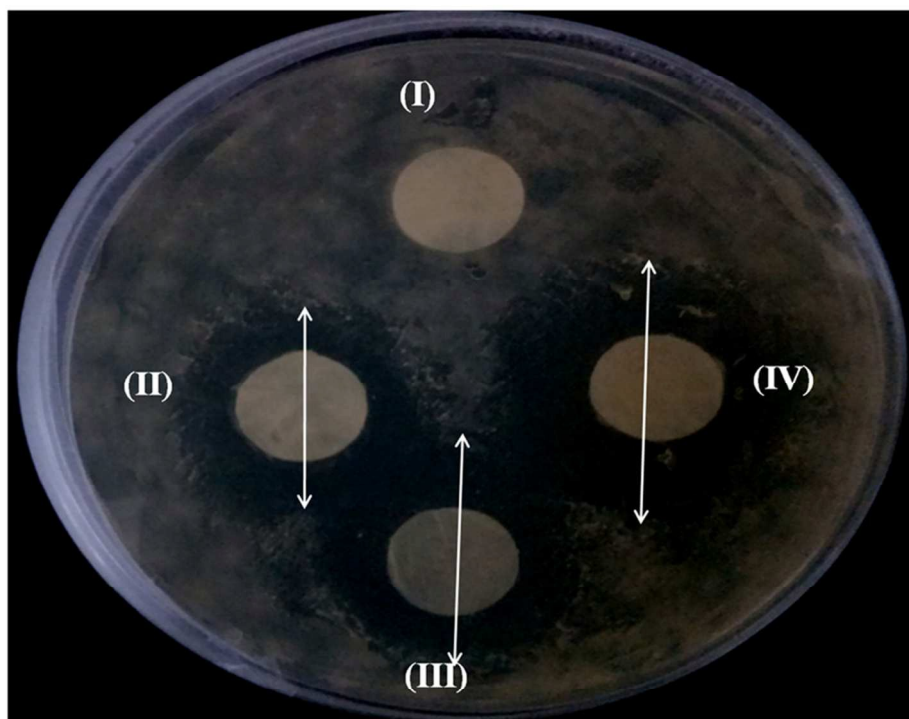
95x73mm (300 x 300 DPI)
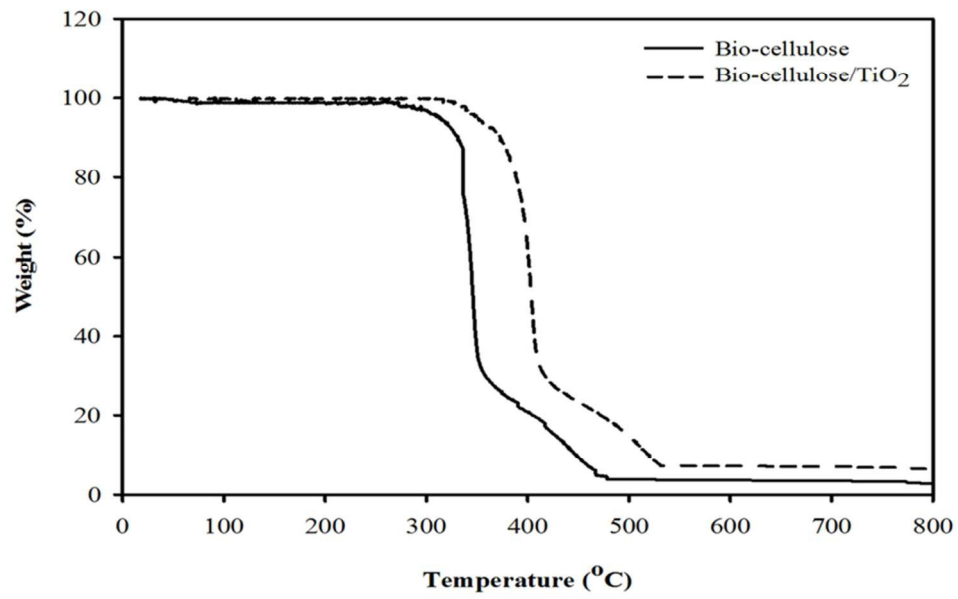
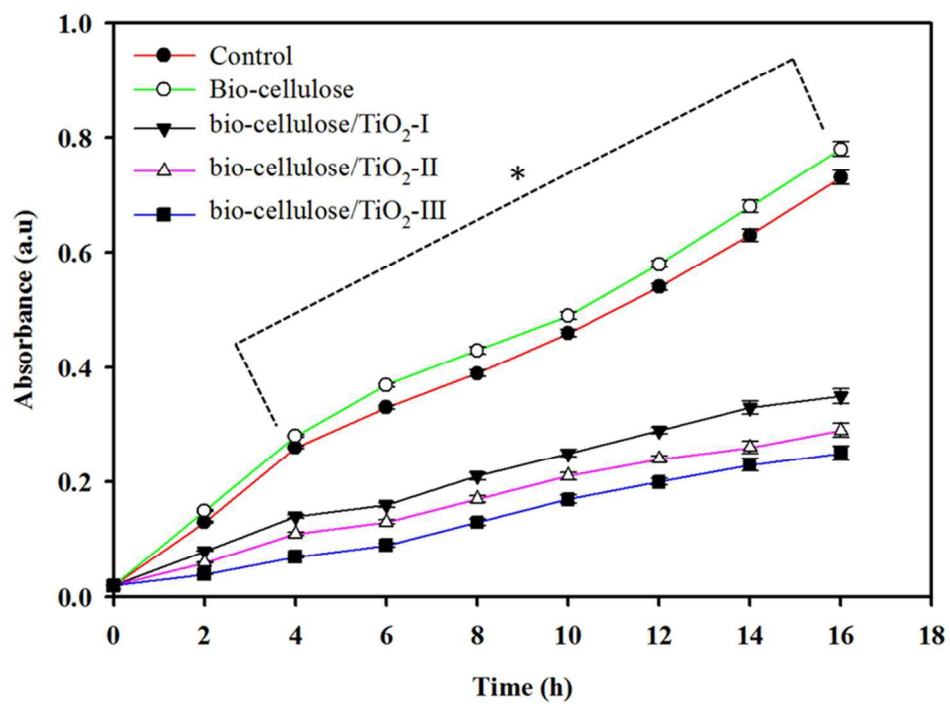Ullah et al., Fig. 4A

96x73mm (300 x 300 DPI)
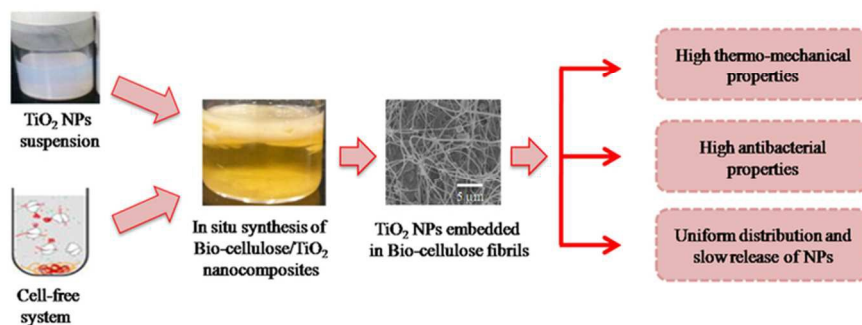
Ullah et al., Fig. 4B

93x75mm (300 x 300 DPI)

Ullah et al., Fig. 5A

96x88mm (300 x 300 DPI)

Ullah et al., Fig. 5B

92x80mm (300 x 300 DPI)

Ullah et al., Graphical Abstract

74x39mm (300 x 300 DPI)